

The Inhibited effect of Phenolphthalein towards the corrosion of C38 Steel in Hydrochloric Acid

D. Ben Hmamou¹, R. Salghi^{1,*}, A. Zarrouk², H. Zarrok³, S. S. Al-Deyab⁴, O. Benali⁵, B. Hammouti^{2,4}

¹ Equipe de Génie de l'Environnement et de Biotechnologie, ENSA, Université Ibn Zohr, BP 1136 Agadir, Morocco

² LCAE-URAC18, Faculté des Sciences, Université Mohammed Premier, BP 4808, Oujda, Morocco.

³ Laboratoire des procédés de séparation, Faculté des Sciences, Kénitra, Morocco

⁴ Petrochemical Research Chair, Department of Chemistry - College of Science, King Saud University, B.O. 2455 Riaydh 11451 Saudi Arabia.

⁵ Département de Biologie, Faculté des Sciences et de la Technologie, Université de Tahar Moulay Saïda, Algérie.

*E-mail: r_salghi@yahoo.fr

Received: 19 July 2012 / Accepted: 21 August 2012 / Published: 1 September 2012

The inhibition of the corrosion of carbon steel in 1 M HCl by Phenolphthalein (Ph) has been investigated in relation to the concentration of the inhibitor as well as the temperature using weight loss and electrochemical measurements. The effect of the temperature on the corrosion behaviour with addition of optimal concentration of Ph was studied in the temperature range 298-323K. Polarisation curves reveal that Ph is a mixed type inhibitor. The value of inhibition efficiency decreases slightly with the increase in the temperature. Changes in impedance parameters (charge transfer resistance, R_t , and double layer capacitance, C_{dl}) were indicative of adsorption of Ph on the metal surface, leading to the formation of a protective film. Adsorption of Ph on the C38 steel surface is found to obey the Langmuir adsorption isotherm. Some thermodynamic functions of dissolution and adsorption processes were also determined.

Keywords: C38 steel, Phenolphthalein (**Ph**), Hydrochloric acid, Adsorption.

1. INTRODUCTION

The corrosion of steel is a fundamental academic and industrial concern that has received a considerable amount of attention. The use of inhibitor is one of the most practical methods to protect metals from corrosion, especially in aggressive media [1-4]. The effect of organic nitrogen compounds

on the corrosion behaviour of metallic materials in aggressive solutions has been well documented [5–25]. The adsorption of the organic inhibitor at the metal solution interface is the first step in the mechanism of the inhibitory action. Organic molecules may adsorb on the metal surface by (a) Electrostatic interaction between a negatively charged surfaces, which is provided with specifically adsorbed anions (Cl^-) on metal and positive charge of the inhibitor. (b) Interaction of unshared electron pair in the inhibitor molecule with metal. (c) Interaction of π electron of the inhibitor molecule with the metal and/or (d) A combination of all the above processes.

In this work, a phenolphthalein containing oxygen and aromatic ring had been studied on the corrosion inhibition of C38 steel in 1M HCl solutions by weight loss and electrochemical methods studies. Figure 1 shows the molecular structure of the investigated compound, which has been labelled **Ph**.

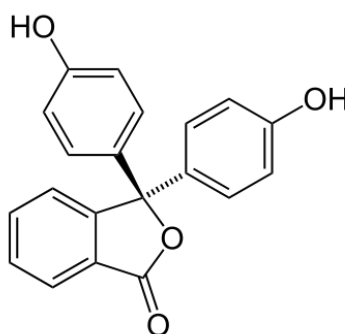


Figure 1. The molecular structure of Phenolphthalein (**Ph**)

2. MATERIALS AND METHODS

2.1. Weight loss measurements

Coupons were cut into $2 \times 2 \times 0.08 \text{ cm}^3$ dimensions having composition (0.179% C, 0.165% Si, 0.439% Mn, 0.203% Cu, 0.034% S and Fe balance) are used for weight loss measurements. Prior to all measurements, the exposed area was mechanically abraded with 180, 320, 800, 1200 grades of emery papers. The specimens are washed thoroughly with bidistilled water, degreased and dried with ethanol. Gravimetric measurements are carried out in a double walled glass cell equipped with a thermostated cooling condenser. The solution volume is 80 cm^3 . The immersion time for the weight loss is 6 h at 298 K.

2.2. Electrochemical tests

The electrochemical study was carried out using a potentiostat PGZ100 piloted by Voltmaster software. This potentiostat is connected to a cell with three electrode thermostats with double wall

(Tacussel Standard CEC/TH). A saturated calomel electrode (SCE) and platinum electrode were used as reference and auxiliary electrodes, respectively. The material used for constructing the working electrode was the same used for gravimetric measurements. The surface area exposed to the electrolyte is 0.094 cm^2 .

Potentiodynamic polarization curves were plotted at a polarization scan rate of 0.5 mV/s . Before all experiments, the potential was stabilized at free potential during 30 min. The polarisation curves are obtained from -800 mV to -400 mV at 298 K . The solution test is there after de-aerated by bubbling nitrogen. Gas bubbling is maintained prior and through the experiments. In order to investigate the effects of temperature and immersion time on the inhibitor performance, some test were carried out in a temperature range $298\text{--}328 \text{ K}$.

The electrochemical impedance spectroscopy (EIS) measurements are carried out with the electrochemical system (Tacussel), which included a digital potentiostat model Voltalab PGZ100 computer at E_{corr} after immersion in solution without bubbling. After the determination of steady-state current at a corrosion potential, sine wave voltage (10 mV) peak to peak, at frequencies between 100 kHz and 10 mHz are superimposed on the rest potential. Computer programs automatically controlled the measurements performed at rest potentials after 0.5 hour of exposure at 298 K . The impedance diagrams are given in the Nyquist representation. Experiments are repeated three times to ensure the reproducibility.

2.3. Solutions preparation

The aggressive solution (1 M HCl) was prepared by dilution of Analytical Grade 37% HCl with distilled water. The organic compound tested is phenolphthalein. The concentration range of this compound was 10^{-2} to 10^{-5} M .

3. RESULTS AND DISCUSSION

3.1. Effect of concentration

3.1.1 Polarization curves

Figure 2 shows the polarization curves of C38 steel in 1 M HCl blank solution and in the presence of different concentrations (10^{-2} to 10^{-5} M) of **Ph**. With the increase of **Ph** concentrations, both anodic and cathodic currents were inhibited. This result shows that the addition of **Ph** inhibitor reduces anodic dissolution and also retards the hydrogen evolution reaction.

For anodic polarization, it can be seen from Fig. 2 that, in the presence of **Ph** at high concentrations, two linear portions were observed. When the anodic potentials increases, the anodic current increases at a slope of b_{a1} in the low polarization potential region. After passing a certain potential E_u , the anodic current increases rapidly and dissolves at a slope of b_{a2} in the high polarization region.

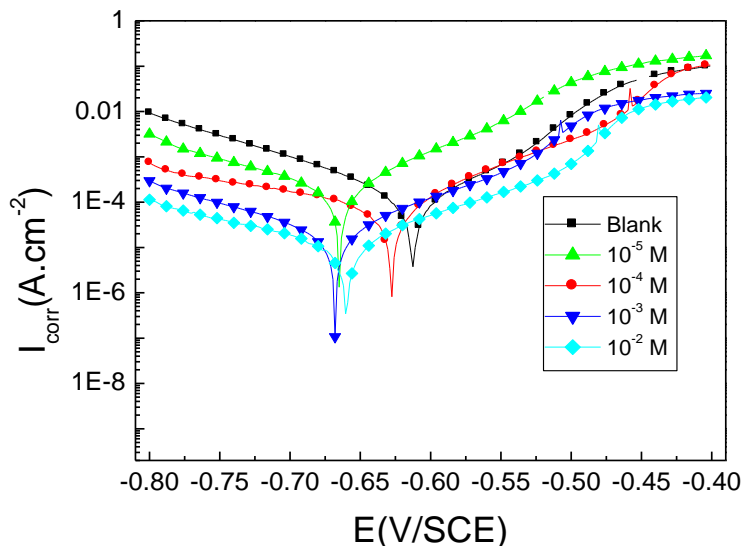


Figure 2. Potentiodynamic polarisation curves of C38 steel in 1M HCl in the presence of different concentrations of **Ph**.

The rapid increase of anodic current after E_u may be due to desorption of **Ph** molecules adsorbed on the electrode. This means that the inhibition mode of **Ph** depends on electrode potential. In this case, the observed inhibition phenomenon is generally described as corrosion inhibition of the interface associated with the formation of a bidimensional layer of adsorbed inhibitor species at the electrode surface [26]. Note that the potential E_u is also denoted E_1 in Bartos and Hackerman’s paper [27].

The inhibition efficiencies were calculated from I_{corr} values according to following equation:

$$P\% = \frac{I_{corr} - I'_{corr}}{I_{corr}} \times 100 \tag{1}$$

Where I_{corr} and I'_{corr} are the corrosion current densities in the absence and the presence of the inhibitor.

Table 1. Electrochemical parameters of C38 steel at various concentrations of **Ph** in 1 M HCl and corresponding inhibition efficiency.

Conc. (M)	E_{corr} (mV/SCE)	I_{corr} ($\mu\text{A}/\text{cm}^2$)	$-b_c$ (mV/dec)	E (%)
Blank	-612	124	174	-
1×10^{-2}	-661	19	136	84.67
1×10^{-3}	-669	36	130	70.96
1×10^{-4}	-666	56	132	54.83
1×10^{-5}	-627	67	135	45.96

Table 1 gives the values of kinetic corrosion parameters as the corrosion potential E_{corr} , corrosion current density I_{corr} , cathodic Tafel slope (b_c), and inhibition efficiency for the corrosion of C38 steel in 1 M HCl with different concentrations of **Ph**. The corrosion current densities were estimated by Tafel extrapolation of the cathodic curves to the open circuit corrosion potentials.

From this table, it can be concluded that:

- The E_{corr} values were shifted toward the negative in the presence of the inhibitor. The presence of **Ph** in the acidic solution results in a slight shift of corrosion potential towards more negative in comparison to that in its absence, and the values of corrosion potential nearly remain constant with the addition of different concentration of **Ph**. These results indicate that **Ph** acts as a mixed-type inhibitor with predominant cathodic effectiveness. According to Ferreira and others [28-29], if the displacement in (E_{corr}) values (i) >85 mV in inhibited system with respect to uninhibited, the inhibitor could be recognized as cathodic or anodic type and (ii) if displacement in E_{corr} is <85 mV, it could be recognized as mixed-type. For studied inhibitors, the maximum displacement range was 57 mV towards cathodic region, which indicates that the studied **Ph** is mixed-type inhibitors [30-31].

- The cathodic Tafel slopes were found to vary over a range of 130 - 174 mV dec^{-1} .

Therefore, the cathodic slope value was found to change with increasing concentration of **Ph** in 1 M HCl. This result indicates the influence of the inhibitor on the kinetics of the hydrogen evolution reaction. Behavior of this type has been observed for mild steel in hydrochloric acid and sulphuric acid solutions containing 3,5-bis(4-methylthiophenyl)-4H-1,2,4-triazole [32] and 1-Methyl-2-Mercapto Imidazole [33].

- The I_{corr} values decreased in the presence of different concentrations of **Ph**.
- Values of inhibition efficiency were found to increase with increase in the concentration of **Ph** reaching maximum value at 10^{-2} M.

3.1.2. Electrochemical impedance spectroscopy measurements

The corrosion behaviour of C38 steel in 1 M HCl in the absence and the presence of **Ph** was investigated by EIS at 298 K after immersion of 0.5 h. A typical set of Nyquist plots for C38 steel in uninhibited and inhibited 1 M HCl is shown in Fig. 3 that impedance spectra show that a single semicircle and the diameter of semicircle increases with increasing inhibitor concentration. These diagrams exhibit that the impedance spectra consist of one capacitive loop at high frequency, the high frequency capacitive loop was attributed to charge transfer of the corrosion process.

To describe the observed depression of the capacitive semicircle it is necessary to replace the capacitor by some element, which has frequency dispersion like the constant phase element (CPE). This element is a generalised tool, which can reflect exponential distribution of the parameters of the electrochemical reaction related to energetic barrier at charge and mass transfer, as well as impedance behaviour caused by fractal surface structure [34].

The dispersion of the capacitive semicircle is explained also by surface heterogeneity due to surface roughness, impurities or dislocations [35-36], distribution of activity centres, inhibitors adsorption and formation of porous layers [37-40]. The impedance of the CPE is [41-42] :

$$Z_{CPE} = Q^{-1} (j\omega)^{-n} \tag{2}$$

where Q is a proportionality coefficient and n an exponent related to the phase shift. For whole numbers of $n = 1, 0, -1$, CPE is reduced to the classical lumped elements capacitor (C), resistance (R) and inductance (L), respectively. The value of $n = 0.5$ corresponds to Warburg impedance (W). Values of n can serve as a measure of the surface heterogeneity [35-36, 43].

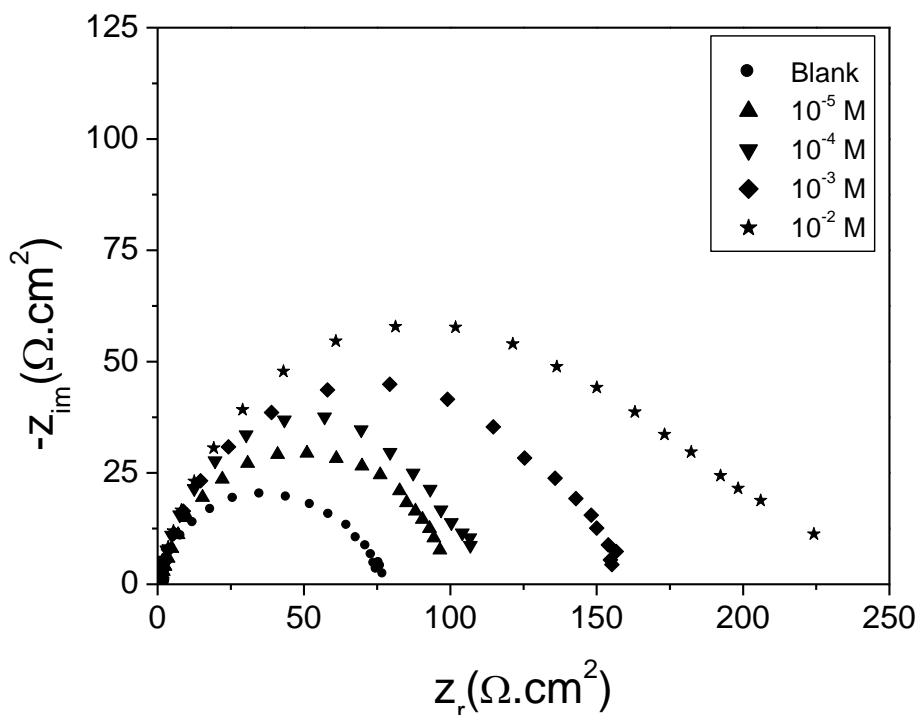


Figure 3. Nyquist diagrams for C38 steel electrode with and without **Ph** at E_{corr} after 30 min of immersion.

The equivalent circuit model employed for these systems is presented in Fig. 4.

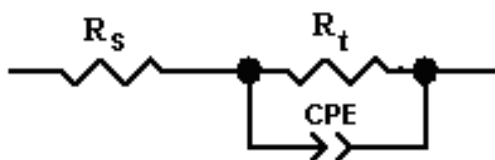


Figure 4. The equivalent circuit of the impedance spectra obtained for **Ph**

The resistance R_s is the resistance of the solution; R_t reflects the charge transfer resistance and CPE has the meaning of a frequency distributed double - layer capacitance.

The percent inhibition efficiency is calculated by charge transfer resistance obtained from Nyquist plots, according to the equation:

$$P \% = \frac{R'_t - R_t}{R'_t} \times 100 \tag{3}$$

where R_t and R'_t are the charge transfer resistance values without and with inhibitor, respectively.

Values of elements of the circuit corresponding to different corrosion systems, including values of C_{dl} , are listed in Table 2.

Table 2. Electrochemical impedance parameters for corrosion of C38 steel in acid medium at various contents of Ph.

Conc. (M)	R_t ($\Omega.cm^2$)	n	$Q(s^n/\Omega.cm^2)$	C_{dl} ($\mu F/cm^2$)	E_{Rt} (%)
Blank	51.4	0.89	1.91×10^{-4}	107.86	----
1×10^{-2}	258.8	0.89	3.07×10^{-5}	16.89	80.14
1×10^{-3}	170.4	0.87	2.73×10^{-5}	12.24	69.83
1×10^{-4}	115.5	0.84	3.43×10^{-5}	11.96	55.50
1×10^{-5}	87.0	0.77	4.35×10^{-5}	8.22	40.91

From this table we can see that, the R_t values of investigated product increase with increasing inhibitor concentration. The greatest effect was observed at a concentration of 10^{-2} M, which produced R_t value of $258.8 \Omega.cm^2$. At the same time the C_{dl} has opposite trend at the whole concentration range. These observations clearly bring out the fact that the corrosion of C38 steel in 1 M HCl is controlled by a charge transfer process. The decrease in C_{dl} is due to the gradual replacement of water molecules by the adsorption of the organic molecules at metal/solution interface, leading to a protective film on the C38 steel surface, and then decreasing the extent of dissolution reaction [44]. The decrease of the values of n when compared with 1 M HCl and with concentration can be explained by some increase of surface heterogeneity, due to the adsorption of the inhibitor on the most active desorption sites [36].

Note that the capacitances were calculated from Q and R_t using the equation [45-46] :

$$Q = \frac{(C R_t)^n}{R_t} \tag{4}$$

3.1.3. Weight loss, corrosion rates and inhibition efficiency

Values of the inhibition efficiency and corrosion rate obtained from the weight loss measurements of C38 steel for different concentrations of inhibitor in 1 M HCl at 298 K after 6 hours of immersion are given in table 3.

Inhibition efficiency E_w (%) is calculated as follows:

$$P \% = \frac{W_{\text{corr}} - W'_{\text{corr}}}{W_{\text{corr}}} \times 100 \quad (5)$$

where W_{corr} and W'_{corr} are the corrosion rates of C38 steel due to the dissolution in 1 M HCl in the absence and the presence of definite concentration of inhibitor, respectively.

This shows that the inhibition efficiency increases with the increasing inhibitor concentration. At this purpose, one observes that the optimum concentration of inhibitor required to achieve the efficiency is found to be 10^{-2} M ($P=84\%$).

Table 3. Effect of **Ph** concentration on corrosion data of C38 steel in 1M HCl

Conc. (M)	W_{corr} (mg. cm ⁻²)	E_w (%)
Blank	1.2614	-
1×10^{-2}	0.2018	84.0
1×10^{-3}	0.3494	72.3
1×10^{-4}	0.5257	58.3
1×10^{-5}	0.6496	48.5

The inhibition of corrosion of C38 steel by **Ph** can be explained in terms of adsorption on the metal surface. This compound can be adsorbed on the metal surface by the interaction between lone pairs of electrons of nitrogen and sulfur atoms of the inhibitor and the metal surface. This process is facilitated by the presence of vacant orbitals of low energy in iron atom, as observed in the transition group metals.

These results are in reasonably good agreement with the values of inhibitor efficiency obtained from electrochemical techniques.

3.2. Adsorption

Basic information on the interaction between the inhibitor and the C38 steel can be provided by the adsorption isotherm. The adsorption of the organic compounds can be described by two main types of interaction: physical adsorption and chemisorption. These are influenced by the chemical structure of the inhibitor, the type of the electrolyte and the charge and nature of the metal.

Surface coverage was estimated as Eq. (5). The θ values for different inhibitor concentrations at 298 K after 6h of immersion.

Attempts were made to fit θ values to various isotherms including Frumkin, Temkin and Langmiur. By far the best fit was obtained with the Langmiur isotherm. According to this isotherm θ is related to concentration inhibitor C via

$$\theta = \frac{KC}{KC + 1} \quad (7)$$

where K is the equilibrium constant for the adsorption process.

$$\log K = -1,74 - \left(-\frac{\Delta G_{Ads}^0}{2,303RT} \right) \quad (8)$$

where ΔG_A^0 is the free energy of adsorption.

Rearrangement of the equation (7) yields to:

$$\frac{C}{\theta} = \frac{1}{K} + C \quad (9)$$

It was found that Figure 5 (plot of $\frac{\theta}{C}$ versus C) gives straight line with slope equal to 0.99, indicating that the adsorption of compound under consideration on steel / acidic solution interface obeys Langmiur's adsorption.

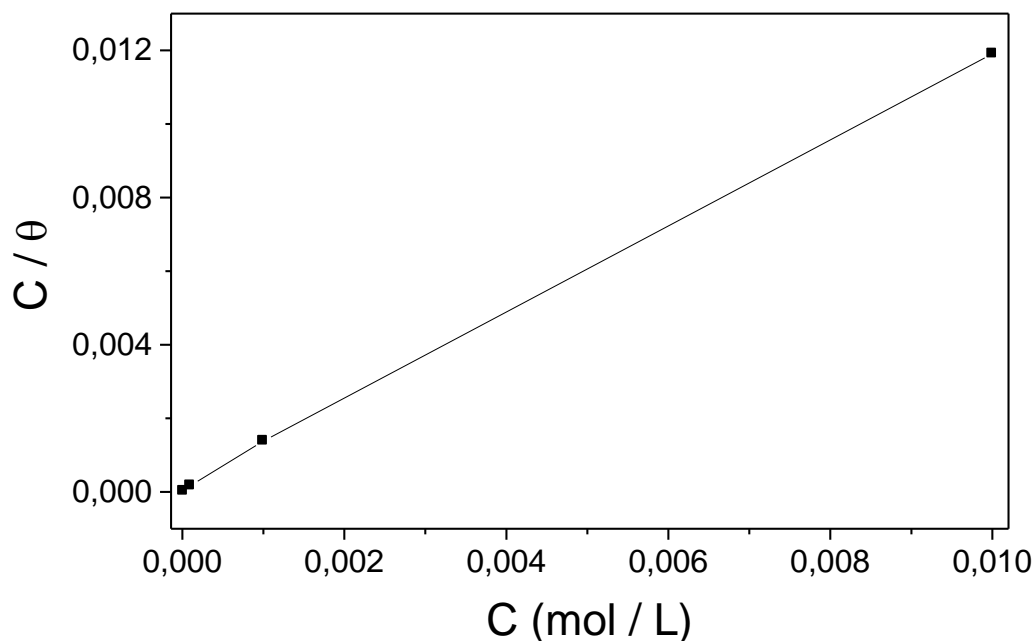


Figure 5. Langmuir isotherm of **Ph** on the C38 steel surface at 298K.

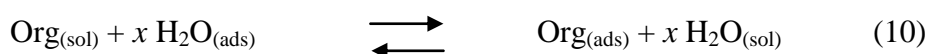
The value of the equilibrium constant, K , for C38 steel in 1 M HCl in the presence of **Ph** is calculated to be 1.19×10^4 L / Mol. The free value of the energy of adsorption as calculated from equation (8) is $\Delta G_{\text{ads}} = -33.21$ kJ/mol.

The negative values of ΔG_{ads}^0 show that the adsorption of **Ph** is a spontaneous process [47] under the experimental conditions described. It is well known that values of $-\Delta G_{\text{ads}}$ of the order of 20 kJ/mol or lower indicate a physisorption; those of order of 40 kJ/mol or higher involve charge sharing or a transfer from the inhibitor molecules to the metal surface to form a co-ordinate type of bond [48-49]. On the other hand, Metikoš-Hukovic *et al.* [50] describe the interaction between thiourea and iron ($\Delta G_{\text{ads}} = -39$ kJ/mol) as chemisorption.

Unlike, Zhang *et al.* [51] consider that the adsorption of 2-(4-pyridyl)-benzimidazole on the mild steel was principally by physisorption occurs together with the chemisorption on the mild steel surface ($\Delta G_{\text{ads}} = -32.37$ kJ/mol).

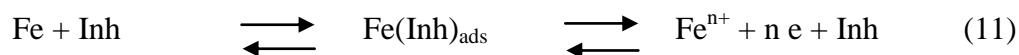
In fact, due to the strong adsorption of water molecules on the surface of mild steel, it may be assumed that adsorption occurs first due to the physical forces, and then the removal of water molecules from the surface is accompanied by chemical interaction between the metal surface and the adsorbate [52].

It should be noted that, the adsorption of an organic adsorbate at a metal solution interface can be represented as a substitutional adsorption process between the organic molecules in the aqueous solution $\text{Org}_{(\text{sol})}$ and the water molecules on the metallic surface $\text{H}_2\text{O}_{(\text{ads})}$ [47].



where $\text{Org}_{(\text{sol})}$ and $\text{Org}_{(\text{ads})}$ are the organic molecules in the aqueous solution and adsorbed on the metallic surface, respectively, $\text{H}_2\text{O}_{(\text{ads})}$ is the water molecules on the metallic surface, x is the size ratio representing the number of water molecules replaced by one molecule of organic adsorbate.

According to Bockris and Drazic [48], the inhibition mechanism could be explained by the $\text{Fe}(\text{inh})_{\text{ads}}$ reaction intermediates :



At first, where there is not enough $\text{Fe}(\text{Inh})_{\text{ads}}$ to cover the metal surface, because the inhibitor concentration is low or because the adsorption rate is slow, metal dissolution takes place on sites of the steel surface free of $\text{Fe}(\text{Inh})_{\text{ads}}$. With high inhibitor concentration, a compact and coherent inhibitor overlayer forms on the steel surface, reducing chemical attack of the metal [49].

3.2. Effect of temperature

To obtain the activation energy of the corrosion process and investigate the effect of temperature, EIS measurements were performed in the temperature range of 298–333 in 1 M HCl solution in the absence and presence of 10^{-2} M **Ph**, as shown in Figs. 6a and 6b.

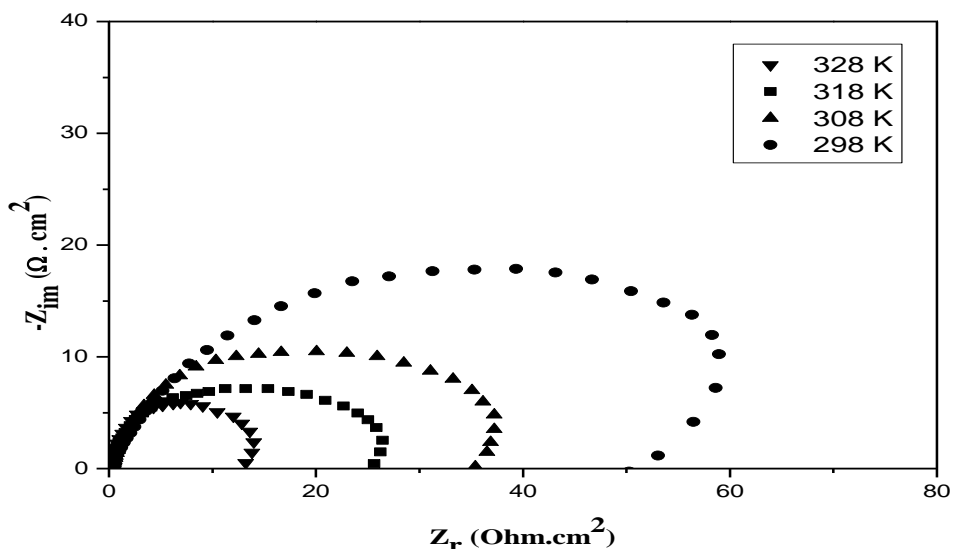


Figure 6a . Nyquist diagrams for C38 steel in 1 M HCl at different temperatures.

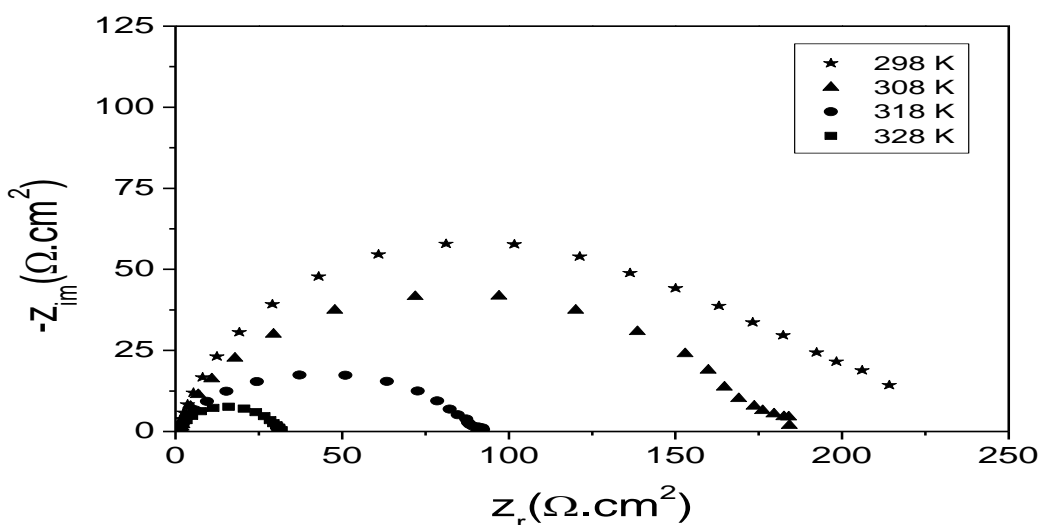


Figure 6b. Nyquist diagrams for C38 steel in 1 M HCl + 10⁻² M of **Ph** at different temperatures.

Electrochemical parameters and inhibition efficiencies are presented in Table 4.

From Figs. 6a and 6b, and Table 4, it can be concluded that the value of R_{tc} values decreases in both uninhibited and inhibited solutions and the value of inhibition efficiency decreases slightly with the increase in the temperature. Thus **Ph** acts as a temperature-dependent inhibitor, and the relationship between temperature and inhibition efficiency is also a characteristic of the physical adsorption [53].

The activation parameters for the corrosion process were calculated from Arrhenius type plot according to the following equation:

$$\log (1/R_{tc}) = -\frac{E_a}{RT} + \log A \tag{12}$$

and from transition state plot according to the following equation:

$$\log \frac{1}{T \cdot R_{tc}} = -\frac{\Delta H_a^0}{R T} + B \tag{13}$$

where E_a is the apparent activation energy, A the pre-exponential factor, R the universal gas constant, ΔH_a the enthalpy of activation and T the absolute temperature.

Table 4. Effect of temperature on the C38 steel in free acid and at 10^{-2} M of **Ph**

	Temperature (K)	R_{tc} ($\Omega \cdot \text{cm}^2$)	n	Q ($\text{s}^n / \Omega \cdot \text{cm}^2$)	C_{dl} ($\mu\text{F} / \text{cm}^2$)	E_{Rt} (%)
HCl	298	51.42	0.89	1.91×10^{-4}	107.88	----
	308	30.25	0.85	1.61×10^{-4}	62.94	----
	318	21.31	0.86	1.31×10^{-4}	50.41	----
	328	12.53	0.88	1.11×10^{-4}	45.20	----
Ph	298	258.8	0.81	3.07×10^{-5}	16.91	80.13
	308	140.3	0.90	1.57×10^{-5}	7.94	78.43
	318	91.66	0.90	1.63×10^{-5}	7.90	76.75
	328	40.82	0.86	2.39×10^{-5}	7.72	69.99

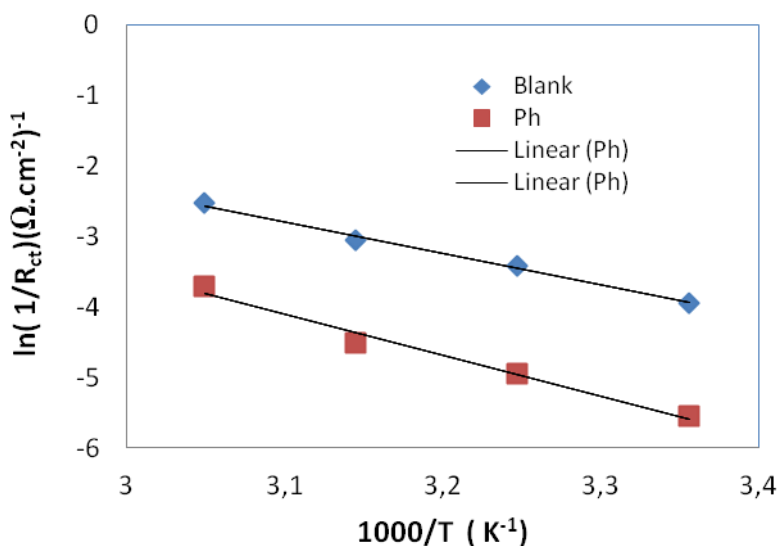


Figure 7a. Arrhenius plots of steel in 1 M HCl with and without 10^{-2} M of **Ph**

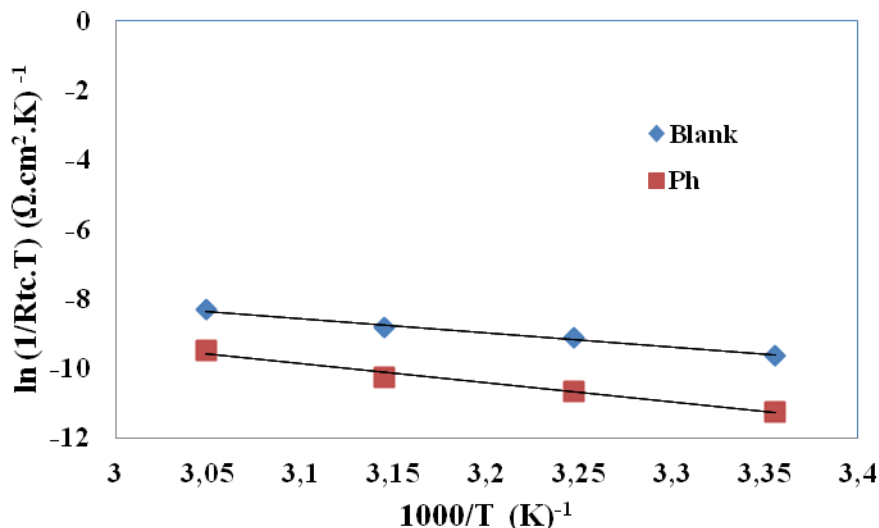


Figure 7b. Relation between $\ln(1/R_{tc}T)$ and $1000/T$ at different temperatures.

The variations of logarithm of the corrosion rate of C38 steel ($\log 1/R_{tc}$) in 1 M HCl containing optimal concentration of **Ph** and $\log (1/(T.R_{tc}))$ with reciprocal of the absolute temperature are presented in Figs. 7a and 7b, respectively. Straight lines with coefficients of correlation (c. c) higher to 0.99 are obtained.

The E_a and ΔH_a values were determined from the slopes of these plots. The calculated values of E_a and ΔH_a in the absence and the presence of 10^{-2} Mol/L of **Ph** are given in Table 5.

Table 5. Values of activation parameters (E_a , ΔH_a and ΔS_a) for C38 steel in 1M HCl in the absence and presence of 10^{-2} M of **Ph**

	E_a (kJ/mol)	ΔH_a (kJ/mol)	ΔS_a (J/mol)	ΔH_a (KJ/mol) from Eq.(14)
Blank	37.22	34.63	-164.35	34.74
Ph	48.33	45.73	-137.78	45.85

The value of E_a in the inhibited solution is higher than that in the uninhibited solution, suggesting that the adsorption mechanism of **Ph** in 1.0 M HCl is typical to physisorption. However, the criteria, in which the increasing activation energy in the presence of inhibitor indicates that physical adsorption occurs in the first stage [54], cannot be taken as decisive due to competitive adsorption with water whose removal from the surface requires also some activation energy [52]. Therefore, the adsorption phenomenon of an organic molecule is not considered only as a physical or as chemical adsorption phenomenon [55]. A wide spectrum of conditions, ranging from the dominance of chemisorption or electrostatic effects arises from other adsorption experimental data [55-56].

Moreover one remark that the ΔH_a values obtained from the slopes of plots $\log (I_{\text{corr}}/ T)$ vs $f(1/T)$ and those determined from the equation (14) are in good agreement.

$$\Delta H_a = E_a - RT \quad (14)$$

4. CONCLUSION

It can be concluded that:

- **Ph** inhibits the corrosion of C38 steel.
- **Ph** acts predominantly as mixed inhibitor
- The concentration dependence of the inhibition efficiency calculated from weight loss measurements and electrochemical studies has the same tendency.
 - Adsorption of **Ph** the steel surface in hydrochloric acid obeys the langmuir adsorption isotherm model and leads to the formation of a protective film.
 - The inhibition efficiency of **Ph** is temperature dependant and inhibition efficiency decreases slightly with the increase in the temperature.
 - The addition of **Ph** leads to a decrease in activation corrosion energy.

ACKNOWLEDGEMENTS

Prof S. S. Al-Deyab, Prof B. Hammouti and Prof R. Salghi extend their appreciation to the Deanship of Scientific Research at King Saud University for funding the work through the research group project No. RGP-VPP-089.

References

1. Khaled, K.F. *Electrochim. Acta.*, 54 (2009) 4345.
2. Mihit, M; Salghi, R.; El Issami, S.; Bazzi, L.; Hammouti, B.; Ait Addi, E.; Kertit, S. *Pigm. Resin Techn.*, 35 (2006) 151.
3. Dafali, A.; Hammouti, B.; Mokhlisse, R.; Kertit, S. *Corros. Sci.*, 45 (2003) 1619.
4. Kertit, S.; Salghi, R.; Bazzi, L.; Hammouti, B.; Bouchart, A. *Ann. Chim. Sci. Mat.*, 25 (2000) 187.
5. D. Ben Hmamou, R. Salghi, A. Zarrouk, H. Zarrok, B. Hammouti, S. S. Al-Deyab, M. Bouachrine, A. Chakir, M. Zougagh, *Int. J. Electrochem. Sci.* 7 (2012) 5716
6. B. Hammouti, R. Salghi and S. Kertit, *J. Electrochem Soc. India.* 47 (1998) 31.
7. H. Zarrok, H. Oudda, A. Zarrouk, R. Salghi, B. Hammouti, M. Bouachrine, *Der Pharma Chemica.* 3 (6) (2011) 576.
8. M. Mihit, S. El Issami, M. Bouklah, L. Bazzi, B. Hammouti, E. Ait Addi, R. Salghi, S. Kertit, *Applied Suf Sci.* 252 (6) (2006) 2389.
9. K. Barouni, L. Bazzi, R. Salghi M. Mihit, B. Hammouti, A. Albourine, S. El Issami, *Mater. Lett.* 62 (2008) 3325.
10. S. El Issami, L. Bazzi, M. Mihit, M. Hilali, R. Salghi, and El. Ait Addi., *J. Phys. IV*, 123 (2005) 307.
11. S. El Issami, L. Bazzi, M. Hilali, R. Salghi, S. Kertit, *Ann. Chim. Sci. Mat.*, 27(2002) 63.

12. S. El Issami, L. Bazzi, M. Mihit, B. Hammouti, S. Kertit, E. Ait Addi, R. Salghi, *Pigment & Resin. Tech.* 36(3) (2007) 161.
13. R. Salghi, L. Bazzi, B. Hammouti and S. Kertit., *Bull. of Electrochem.* 16 (6) (2000) 272.
14. M. Mihit, K. Laarej, H. Abou El Makarim, L. Bazzi, R. Salghi, B. Hammouti, *Arabian J. Chem.* 3 (2010) 55.
15. A. Zarrouk, A. Dafali, B. Hammouti, H. Zarrok, S. Boukhris, M. Zertoubi, *Int. J. Electrochem. Sci.* 5 (2010) 46.
16. A. Zarrouk, T. Chelfi, A. Dafali, B. Hammouti, S.S. Al-Deyab, I. Warad, N. Benchat, M. Zertoubi, *Int. J. Electrochem. Sci.* 5 (2010) 696.
17. A. Zarrouk, B. Hammouti, A. Dafali, H. Zarrok, *Der Pharma Chemica.* 3 (4) (2011) 266.
18. A. Zarrouk, B. Hammouti, R. Touzani, S. S. Al-Deyab, M. Zertoubi, A. Dafali, S. Elkadiri, *Int. J. Electrochem. Sci.* 6 (2011) 4939.
19. A. Zarrouk, B. Hammouti, H. Zarrok, *Der Pharma Chemica,* 3 (5) (2011) 263-271.
20. H. Zarrok, R. Saddik, H. Oudda, B. Hammouti, A. El Midaoui, A. Zarrouk, N. Benchat, M. Ebn Touhami, *Der Pharma Chemica,* 3 (5) (2011) 272.
21. A. Zarrouk, B. Hammouti, A. Dafali, H. Zarrok, R. Touzani, M. Bouachrine, M. Zertoubi, *Res. Chem. Intermed.* (2011) DOI 10.1007/s11164-011-0444-2.
22. A. Zarrouk, B. Hammouti, H. Zarrok, M. Bouachrine, K.F. Khaled, S.S. Al-Deyab, *Int. J. Electrochem. Sci.* 6 (2012) 89.
23. A. Zarrouk, B. Hammouti, H. Zarrok, R. Salghi, A. Dafali, Lh. Bazzi, L. Bammou, S. S. Al-Deyab, *Der Pharma Chemica.* 4 (1) (2012) 337.
24. H. Zarrok, R. Salghi, A. Zarrouk, B. Hammouti, H. Oudda, Lh. Bazzi, L. Bammou, S. S. Al-Deyab, *Der Pharma Chemica.* 4 (1) (2012) 407.
25. H. Zarrok, H. Oudda, A. El Midaoui, A. Zarrouk, B. Hammouti, M. Ebn Touhami, A. Attayibat, S. Radi, R. Touzani, *Res. Chem. Intermed.*, (2012) DOI: 10.1007/s11164-012-0525-x).
26. W. J. Lorentz, F. Mansfeld, *Corro. Sci.* 31(1986) 467.
27. M. Bartos, N. Hackerman, *J. Electrochem. Soc.* 139 (2000) 3428.
28. E.S. Ferreira, C. Giancomelli, F.C. Giacomelli, A. Spinelli, *Mater. Chem. Phys.* 83 (2004) 129.
29. W.H. Li, Q. He, C.L. Pei, B.R. Hou, *J. Appl. Electrochem.* 38 (2008) 289.
30. H.A. Sorkhabi, B. Shaabani, D. Seifzadeh, *Appl. Surf. Sci.* 239 (2005) 154.
31. D. K. Yadav, B. Maiti, M.A. Quraishi, *Corros. Sci.* 52 (2010) 3586.
32. M. Lagrenée, B. Mernari, M. Bouanis, M. Traisnel, F. Bentiss, *Corros. Sci.* 44 (2002) 573.
33. O. Benali, L. Larabi, B. Tabti, Y. Harek, *Anti-Corros. Meth. Mater.* 52 (2005) 280.
34. A. Popova, M. Christov, *Corros. Sci.* 48 (2006) 3208.
35. Z. B. Stoynov, B. M. Grafov, B. Savova-Stoynova, V. V. Elkin, *Electrochemical Impedance*, Nauka, Moscow, 1991.
36. F. B. Growcock, R. J. Jasinski, *J. Electrochem. Soc.* 136 (1989) 2310.
37. U. Rammelt, G. Reinhard, *Corros. Sci.* 27 (1987) 373.
38. O. Benali, L. Larabi, S. M. Mekelleche, Y. Harek, *J. Mater. Sci.* 41 (2006) 7064.
39. S. Merah, L. Larabi, O. Benali, Y. Harek, *Pig. Res. Tech.* 37(5), 291 (2008).
40. O. Benali, L. Larabi, Y. Harek, *J. App. Electrochem.* 39 (2009) 769.
41. Z. Stoynov, *Electrochim. Acta* 35 (1990) 1493.
42. J. R. Macdonald, *J. Electroanal. Chem.* 223 (1987) 233.
43. D. A. Lopez, S. N. Simison, S. R. De Sanchez, *Electrochim. Acta* 48 (2003) 845.
44. C. Selles, O. Benali, B. Tabti, L. Larabi, Y. Harek, *J. Mater. Environ. Sci.* 3 (1) (2012) 206.
45. X. Wu, H. Ma, S. Chen, Z. Xu, A. Sui, *J. Electrochem. Soc.* 146 (1999) 1847.
46. H. Ma, S. Chen, B. Yin, S. Zhao, X. Liu, *Corros. Sci.* 45 (2003) 867.
47. J. O'M Bockris, D. A. J. Swinkels, *J. Electrochem. Soc.* 111 (1964) 736.
48. J. O'M Bockris, D. Drazic, *Electrochim. Acta* 7 (1962) 293.
49. V. Branzoi, F. Branzoi, M. Baibarac, *Mater. Chem. Phys.* 65 (2000) 288.

50. A. Y. El- Etre, *Corros. Sci.* 43 (2001) 1031.
51. F. Zhang, Y. Tang, Z. Cao, W. Jing, Z. Wua, Y. Chen, *Corros. Sci.* 61 (2012) 1.
52. L. M. Vracar, D. M. Drazic, *Corros. Sci.* 44 (2002) 1669.
53. R. Solmaz, G. Kardas, M. Çulha, B. Yazici, M. Erbil, *Electrochim. Acta* 53 (2008) 5941.
54. M. S. Morad, A. M. K. El-Dean, *Corros. Sci.* 48 (2006) 3398.
55. R. Solmaz, G. Kardas, B. Yazici, M. Erbil, *Colloids Surf., A* 312 (2008) 7.
56. I. El Ouali, B. Hammouti, A. Aouniti, Y. Ramli, M. Azougagh, E.M. Essassi, M. Bouachrine *J. Mater. Environ. Sci.* 1 (2010) 4.